

Finite-Volume Electromagnetic Corrections to the Masses of Mesons, Baryons and Nuclei

Zohreh Davoudi^{*1,2} and Martin J. Savage^{†1,2}

¹*Department of Physics, University of Washington, Box 351560, Seattle, WA 98195, USA*

²*Institute for Nuclear Theory, Box 351550, Seattle, WA 98195-1550, USA*

(Dated: July 10, 2018 - 4:28)

Now that Lattice QCD calculations are beginning to include QED, it is important to better understand how hadronic properties are modified by finite-volume QED effects. They are known to exhibit power-law scaling with volume, in contrast to the exponential behavior of finite-volume strong interaction effects. We use non-relativistic effective field theories describing the low-momentum behavior of hadrons to determine the finite-volume QED corrections to the masses of mesons, baryons and nuclei out to $\mathcal{O}(1/L^4)$ in a volume expansion, where L is the spatial extent of the cubic volume. This generalizes the previously determined expansion for mesons, and extends it by two orders in $1/L$ to include contributions from the charge radius, magnetic moment and polarizabilities of the hadron. We make an observation about direct calculations of the muon $g - 2$ in a finite volume.

I. INTRODUCTION

Lattice Quantum Chromodynamics (LQCD) has matured to the point where basic properties of the light hadrons are being calculated at the physical pion mass [1–5]. In some instances, the up- and down-quark masses and quenched Quantum Electrodynamics (QED) have been included in an effort to precisely predict the observed isospin splittings in the spectrum of hadrons [4, 6–14]. While naively appearing to be a simple extension of pure LQCD calculations, there are subtleties associated with including QED. In particular, Gauss’s law and Ampere’s law cannot be satisfied when the electromagnetic gauge field is subject to periodic boundary conditions (PBCs) [15–17]. However, a uniform background charge density can be introduced to circumvent this problem and restore these laws. This is equivalent to removing the zero modes of the photon in a finite-volume (FV) calculation, which does not change the infinite-volume value of calculated quantities. One-loop level calculations in chiral perturbation theory (χ PT) and partially-quenched χ PT ($PQ\chi$ PT) have been performed [17] to determine the leading FV modifications to the mass of mesons induced by constraining QED to a cubic volume subject to PBCs. ¹ Due to the photon being massless, the FV QED corrections to the mass of the π^+ are predicted to be an expansion in powers of the volume, and have been determined to be of the form $\delta m_{\pi^+} \sim 1/L + 2/(m_{\pi^+}L^2) + \dots$, where L is the spatial extent of the cubic volume. As the spatial extents of present-day gauge-field configurations at the physical pion mass are not large, with $m_{\pi}L \lesssim 4$, the exponentially suppressed strong interaction FV effects, $\mathcal{O}(e^{-m_{\pi}L})$, are not negligible for precision studies of hadrons, and when QED is included, the power-law corrections, although suppressed by α_e , are expected to be important, particularly in mass splittings.

In this work, we return to the issue of calculating FV QED effects, and show that non-relativistic effective field theories (NREFTs) provide a straightforward way to calculate such corrections to the properties of hadrons. With these EFTs, the FV mass shift of mesons, baryons and nuclei are calculated out to $\mathcal{O}(1/L^4)$ in the $1/L$ expansion, including contributions from their charge radii,

* davoudi@uw.edu

† mjs5@uw.edu

¹ Vector dominance [18] has been previously used to model the low-momentum contributions to the FV electromagnetic mass splittings of the pseudo-scalar mesons, see Refs. [6, 16].

magnetic moments and polarizabilities. The NREFTs have the advantage that the coefficients of operators coupling to the electromagnetic field are directly related, order by order in the α_e , to the electromagnetic moments of the hadrons (in the continuum limit), as opposed to a perturbative estimate thereof (as is the case in χ PT). For protons and neutrons, the NREFT is the well-established non-relativistic QED (NRQED) [19–27], modified to include the finite extent of the charge and current densities [28]. Including multi-nucleon interactions, this framework has been used extensively to describe the low-energy behavior of nucleons and nuclear interactions, EFT(\not{A}), along with their interactions with electromagnetic fields [28–33], and is straightforwardly generalized to hadrons and nuclei with arbitrary angular momentum. LQCD calculations performed with background electromagnetic fields are currently making use of these NREFTs to extract the properties of hadrons, including magnetic moments and polarizabilities [34–45].

II. FINITE-VOLUME QED

The issues complicating the inclusion of QED in FV calculations with PBCs are well known, the most glaring of which is the inability to preserve Gauss’s law [6, 16, 17], which relates the electric flux penetrating any closed surface to the charge enclosed by the surface, and Ampere’s Law, which relates the integral of the magnetic field around a closed loop to the current penetrating the loop. An obvious way to see the problem is to consider the electric field along the axes of the cubic volume (particularly at the surface) associated with a point charge at the center. Restating the discussions of Ref. [17], the variation of the QED action is, for a fermion of charge eQ ,

$$\begin{aligned} \delta S &= \int d^4x \left[\partial_\mu F^{\mu\nu}(x) - e Q \bar{\psi}(x) \gamma^\nu \psi(x) \right] \delta(A_\nu(x)) \\ &= \int dt \frac{1}{L^3} \sum_{\mathbf{q}} \delta\left(\tilde{A}_\nu(t, \mathbf{q})\right) \int_{L^3} d^3\mathbf{x} e^{i\mathbf{q}\cdot\mathbf{x}} \left[\partial_\mu F^{\mu\nu}(t, \mathbf{x}) - e Q \bar{\psi}(t, \mathbf{x}) \gamma^\nu \psi(t, \mathbf{x}) \right], \quad (1) \end{aligned}$$

where $\tilde{A}_\nu(t, \mathbf{q})$ is the spatial Fourier transform of $A_\nu(t, \mathbf{x})$, and $e = |e|$ is the magnitude of the electronic charge. For simplicity, here and in what follows, we assume the time direction of the FV to be infinite² while the spatial directions are of length L . Eq. (1) leads to $\partial_\mu F^{\mu\nu} = eQ\bar{\psi}\gamma^\nu\psi$ for $\delta S = 0$ and hence Gauss’s Law and Ampere’s Law. This can be modified to $\partial_\mu F^{\mu\nu} = eQ\bar{\psi}\gamma^\nu\psi + b^\nu$ simply by omitting the spatial zero modes of A_μ , i.e. $\tilde{A}_\nu(t, \mathbf{0}) = 0$, or more generally by setting $\delta\tilde{A}_\nu(t, \mathbf{0}) = 0$, where b^ν is some uniform background charge distribution [9].³ This readily eliminates the relation between the electric flux penetrating a closed surface and the inserted charge, and the analogous relation between the magnetic field and current.⁴ Ensuring this constraint is preserved under gauge transformations, $A_\mu(t, \mathbf{x}) \rightarrow A'_\mu(t, \mathbf{x}) = A_\mu(t, \mathbf{x}) + \partial_\mu\Lambda(t, \mathbf{x})$, where Λ is a periodic function in the spatial volume, requires $\partial_0\tilde{\Lambda}(t, \mathbf{0}) = 0$, where $\tilde{\Lambda}(t, \mathbf{q})$ is the Fourier transform of $\Lambda(t, \mathbf{x})$. Modes with $\mathbf{q} \neq \mathbf{0}$ are subject to the standard gauge-fixing conditions, and in LQCD calculations it is sometimes convenient to work in Coulomb gauge, $\nabla \cdot \mathbf{A} = 0$. This is because of the asymmetry between the spatial and temporal directions that is present in most ensembles of gauge field configurations, along with the fact that the photon fields are generated in momentum space as opposed to position space [6].

² In practice, there are thermal effects in LQCD calculations due to the finite extent of the time direction.

³ The introduction of a uniformly charged background is a technique that has been used extensively to include electromagnetic interactions into calculations of many-body systems, such as nuclear matter and condensed matter, see for example Ref. [46].

⁴ For a discussion about including QED with C-PBCs (anti-PBCs), see Ref. [47].

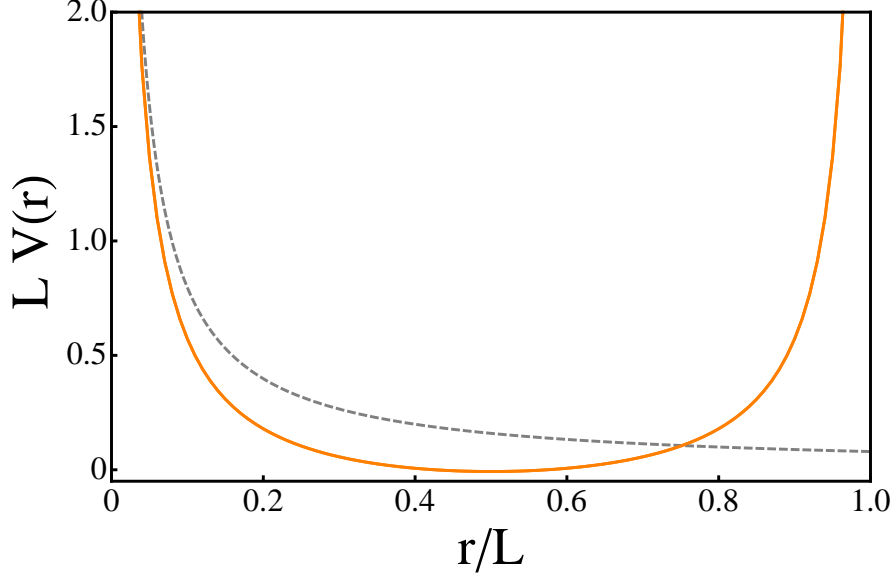


FIG. 1: The FV potential energy between two charges with $Qe = 1$ along one of the axes of a cubic volume of spatial extent L (solid orange curve), obtained from Eq. (2), and the corresponding infinite-volume Coulomb potential energy (dashed gray curve).

In infinite volume, the Coulomb potential energy between charges eQ is well known to be $U(r) = \frac{\alpha_e Q^2}{r}$, where $\alpha_e = e^2/4\pi$ is the QED fine-structure constant, while in a cubic spatial volume with the zero modes removed, it is

$$\begin{aligned}
 U(\mathbf{r}, L) &= \frac{\alpha_e Q^2}{\pi L} \sum_{\mathbf{n} \neq \mathbf{0}} \frac{1}{|\mathbf{n}|^2} e^{\frac{i2\pi \mathbf{n} \cdot \mathbf{r}}{L}} \\
 &= \frac{\alpha_e Q^2}{\pi L} \left[-1 + \sum_{\mathbf{n} \neq \mathbf{0}} \frac{e^{-|\mathbf{n}|^2}}{|\mathbf{n}|^2} e^{\frac{i2\pi \mathbf{n} \cdot \mathbf{r}}{L}} + \sum_{\mathbf{p}} \int_0^1 dt \left(\frac{\pi}{t}\right)^{3/2} e^{-\frac{\pi^2 |\mathbf{p} - \mathbf{r}/L|^2}{t}} \right], \quad (2)
 \end{aligned}$$

where \mathbf{n} and \mathbf{p} are triplets of integers. The latter, exponentially accelerated, expression in Eq. (2) is obtained from the former using the Poisson summation formula. The FV potential energy between two charges with $Qe = 1$, and the corresponding infinite-volume Coulomb potential energy are shown in Fig. 1.

In the next sections, we construct non-relativistic EFTs to allow for order-by-order calculations of the FV QED modifications to the energy of hadrons in the continuum limit of LQCD calculations, going beyond the first two orders in the $1/L$ expansion that have been determined previously. While these EFTs permit calculations to any given precision, including quantum fluctuations, some of the results that will be presented can be determined simply without the EFTs; a demonstration of which is the self-energy of a uniformly charged, rigid and fixed, sphere in a FV. In this textbook case, the self-energy can be determined directly by integrating the interaction between infinitesimal volumes of the charge density, as governed by the modified Coulomb potential, Eq. (2), over the sphere of radius R . It is straightforward to show that the self-energy can be written in an expansion of R/L ,

$$U^{\text{sphere}}(R, L) = \frac{3}{5} \frac{(Qe)^2}{4\pi R} + \frac{(Qe)^2}{8\pi L} c_1 + \frac{(Qe)^2}{10L} \left(\frac{R}{L}\right)^2 + \dots, \quad (3)$$

where $c_1 = -2.83729$ [48–50]. The leading contribution is the well-known result for a uniformly

charged sphere, while the second term, the leading order (LO) FV correction, is independent of the structure of the charge distribution. This suggests that it is also valid for a point particle; a result that proves to be valid for the corrections to the masses of single particles calculated with χ PT and with the NREFTs presented in this work. It is simply the modification to the Coulomb self-energy of a point charge. The third term can be written as $(Qe)^2\langle r^2\rangle/6L^3$, where $\langle r^2\rangle = \frac{3}{5}R^2$ is the mean-squared radius of the sphere, and reproduces the charge-radius contributions determined with the NREFTs, as will be shown in the next section.

III. SCALAR NRQED FOR MESONS AND $J = 0$ NUCLEI

LQCD calculations including QED have been largely focused on the masses of the pions and kaons in an effort to extract the values of electromagnetic counterterms of χ PT, thus we begin by considering the FV corrections to the masses of scalar hadrons. In the limit where the volume of space is much larger than that of the hadron, keeping in mind that only the zero modes are being excluded from the photon fields, the FV corrections to the mass of the hadron will have a power-law dependence upon L , and vanish as $L \rightarrow \infty$. As the modifications to the self-energy arise from the infrared behavior of the theory, low-energy EFT provides a tool with which to systematically determine the FV effects in an expansion in one or more small parameters.

Using the methods developed to describe heavy-quark and heavy-hadron systems [19–26, 28, 45, 51], the Lagrange density describing the low-energy dynamics of a charged composite scalar particle, ϕ , with charge eQ can be written as an expansion in $1/m_\phi$ and in the scale of compositeness,

$$\begin{aligned} \mathcal{L}_\phi = \phi^\dagger \left[iD_0 + \frac{|\mathbf{D}|^2}{2m_\phi} + \frac{|\mathbf{D}|^4}{8m_\phi^3} + \frac{e\langle r^2\rangle_\phi}{6} \nabla \cdot \mathbf{E} + 2\pi\tilde{\alpha}_E^{(\phi)}|\mathbf{E}|^2 + 2\pi\tilde{\beta}_M^{(\phi)}|\mathbf{B}|^2 \right. \\ \left. + iec_M \frac{\{D^i, (\nabla \times \mathbf{B})^i\}}{8m_\phi^3} + \dots \right] \phi, \end{aligned} \quad (4)$$

where m_ϕ is the mass of the particle, the covariant derivative is $D_\mu = \partial_\mu + ie\hat{Q}A_\mu$ with \hat{Q} the charge operator. $\langle r^2\rangle_\phi$ is the mean-squared charge radius of the ϕ , and we have performed the standard field redefinition to the NR normalization of states, $\phi \rightarrow \phi/\sqrt{2m_\phi}$. The remaining coefficients of operators involving the electric, \mathbf{E} , and magnetic, \mathbf{B} , fields, have been determined by matching this EFT to scalar QED, to yield

$$\tilde{\alpha}_E^{(\phi)} = \alpha_E^{(\phi)} - \frac{\alpha_e Q}{3m_\phi} \langle r^2\rangle_\phi, \quad \tilde{\beta}_M^{(\phi)} = \beta_M^{(\phi)}, \quad c_M = \frac{2}{3}m_\phi^2 \langle r^2\rangle_\phi, \quad (5)$$

where $\alpha_E^{(\phi)}, \beta_M^{(\phi)}$ are the electric and magnetic polarizabilities of the ϕ .⁵ These coefficients will be modified at higher orders in perturbation theory, starting at $\mathcal{O}(\alpha_e)$. They will also be modified by terms that are exponentially suppressed by compositeness length scales, e.g. $\sim e^{-m_\pi L}$ for QCD. The ellipses denote terms that are higher order in derivatives acting on the fields, with coefficients dictated by the mass and compositeness scale – the chiral symmetry breaking scale, Λ_χ , for mesons and baryons. For one-body observables, terms beyond $\phi^\dagger i\partial_0\phi$ are treated in perturbation theory, providing a systematic expansion in $1/L$.

⁵ The presence of a charge-radius dependent term in the coefficient of the electric polarizability indicates a subtlety in using this EFT to describe hadrons in a background electric field [45]. Such contributions can be canceled by including redundant operators in the EFT Lagrange density when matching to S-matrix elements. Since a classical uniform electric field modifies the equations of motion, such operators must be retained in the Lagrange density and their coefficients matched directly to Green functions.

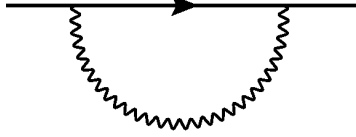


FIG. 2: The one-loop diagram providing the LO, $\mathcal{O}(\alpha_e/L)$, FV correction to the mass of a charged scalar particle. The solid straight line denotes a scalar particle, while the wavy line denotes a photon.

The LO, $\mathcal{O}(\alpha_e/L)$, correction to the mass of a charged scalar particle in FV, δm_ϕ , is from the one-loop diagram shown in Fig. 2. While most simply calculated in Coulomb gauge, the diagram can be calculated in any gauge and, in agreement with previous determinations [17], is

$$\delta m_\phi^{(\text{LO})} = \frac{\alpha_e Q^2}{2\pi L} \sum_{\mathbf{n} \neq 0}^{\wedge} \frac{1}{|\mathbf{n}|^2} = \frac{\alpha_e Q^2}{2L} c_1 \quad , \quad (6)$$

with $c_1 = -2.83729$. The sum, \sum^{\wedge} , represents the difference between the sum over the FV modes and the infinite-volume integral, e.g.,

$$\frac{1}{L^3} \sum_{\mathbf{k} \neq 0}^{\wedge} f(\mathbf{k}) \equiv \frac{1}{L^3} \sum_{\mathbf{k} \neq 0} f(\mathbf{k}) - \int \frac{d^3 \mathbf{k}}{(2\pi)^3} f(\mathbf{k}) \quad , \quad (7)$$

for an arbitrary function $f(\mathbf{k})$, and is therefore finite. This shift is a power law in $1/L$ as expected, and provides a reduction in the mass of the hadron. As the infinite-volume Coulomb interaction increases the mass, and the FV result is obtained from the modes that satisfy the PBCs (minus the zero modes), the sign of the correction is also expected. The result in Eq. (6) is nothing more than the difference between the FV and infinite-volume contribution to the Coulomb self-energy of a charged point particle, as seen from Eq. (2), $U(\mathbf{0}, L)/2$.

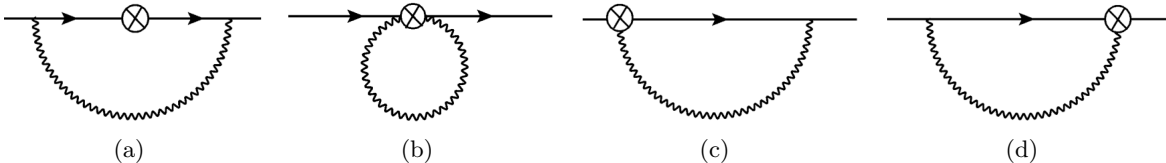


FIG. 3: Diagrams contributing at NLO, $\mathcal{O}(\alpha_e/m_\phi L^2)$, in the $1/L$ expansion. The crossed circle denotes an insertion of the $|\mathbf{D}|^2/2m_\phi$ operator in the scalar QED Lagrange density, Eq. (4).

The next-to-LO (NLO) contribution, $\mathcal{O}(\alpha_e/L^2)$, arises from a single insertion of the $|\mathbf{D}|^2/2m_\phi$ operator in Eq. (4) into the one-loop diagrams shown in Fig. 3. The contribution from each of these diagrams depends upon the choice of gauge, however the sum is gauge independent,⁶

$$\delta m_\phi^{(\text{NLO})} = \frac{\alpha_e Q^2}{m_\phi L^2} \sum_{\mathbf{n} \neq 0}^{\wedge} \frac{1}{|\mathbf{n}|} = \frac{\alpha_e Q^2}{m_\phi L^2} c_1 \quad . \quad (8)$$

⁶ The sums appearing at LO and NLO are

$$\sum_{\mathbf{n} \neq 0}^{\wedge} \frac{1}{|\mathbf{n}|} = c_1 \quad , \quad \sum_{\mathbf{n} \neq 0}^{\wedge} \frac{1}{|\mathbf{n}|^2} = \pi c_1 \quad .$$

This NLO recoil correction agrees with previous calculations [11, 17], and is the highest order in the $1/L$ expansion to which these FV effects have been previously determined.⁷

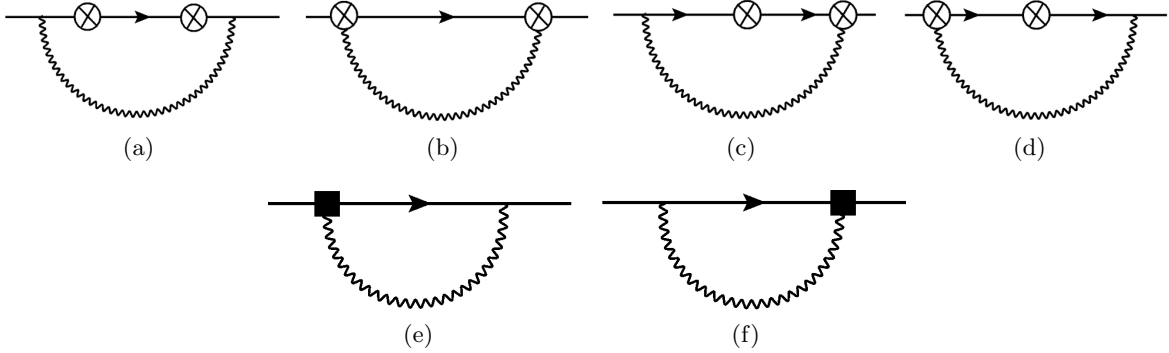


FIG. 4: (a-d) One-loop diagrams giving rise to the recoil corrections of $\mathcal{O}(\alpha_e/m_\phi^2 L^3)$. The crossed circle denotes an insertion of the $|\mathbf{D}|^2/2m_\phi$ operator. (e,f) One-loop diagrams providing the leading contribution from the charge radius of the scalar hadron, $\sim \alpha_e \langle r^2 \rangle_\phi / L^3$. The solid square denotes an insertion of the charge-radius operator in the scalar Lagrange density, Eq. (4).

At next-to-next-to-LO (N²LO), $\mathcal{O}(\alpha_e/L^3)$, there are potentially two contributions – one is a recoil correction of the form $\sim \alpha_e/m_\phi^2 L^3$ and one is from the charge radius, $\sim \alpha_e \langle r^2 \rangle_\phi / L^3$. An evaluation of the one-loop diagrams giving rise to the recoil contributions, Fig. 4(a-d), shows that while individual diagrams are generally non-zero for a given gauge, their sum vanishes in any gauge. Therefore, there are no contributions of the form $\alpha_e/m_\phi^2 L^3$ to the mass of ϕ . In contrast, the leading contribution from the charge radius of the scalar particle, resulting from the one-loop diagrams shown in Fig. 4(e,f) gives a contribution of the form

$$\delta m_\phi^{(\text{N}^2\text{LO})} = -\frac{2\pi\alpha_e Q}{3L^3} \langle r^2 \rangle_\phi \sum_{\mathbf{n} \neq 0}^{\hat{}} 1 = +\frac{2\pi\alpha_e Q}{3L^3} \langle r^2 \rangle_\phi, \quad (9)$$

where $\sum_{\mathbf{n}}^{\hat{}} 1 = 0$.

At N³LO, $\mathcal{O}(\alpha_e/L^4)$, there are potentially three contributions: recoil corrections, $\sim \alpha_e/m_\phi^3 L^4$, contributions from the electric and magnetic polarizability operators, $\sim \tilde{\alpha}_E^{(\phi)}/L^4$, $\tilde{\beta}_M^{(\phi)}/L^4$, and contributions from the c_M operator, Eq. (4). There are two distinct sets of recoil corrections at this order. One set is from diagrams involving three insertions of the $|\mathbf{D}|^2/2m_\phi$ operator, as shown in Fig. 5(a-d), and the other is from a single insertion of the $|\mathbf{D}|^4/8m_\phi^3$ operator, shown in Fig. 5(e,f). The sum of diagrams contributing to each set vanishes, and so there are no contributions of the form $\alpha_e/m_\phi^3 L^4$. The other contributions, which include the electric and magnetic polarizabilities, arise from the one-loop diagrams shown in Fig. 5(g). A straightforward evaluation yields a mass

⁷ The $\mathcal{O}(\alpha_e)$ calculations of Ref. [17] at NLO in χ PT and PQ χ PT do not include the full contributions from the meson charge radius and polarizabilities, but are perturbatively close. This is in contrast to the NREFT calculations presented in this work where the low-energy coefficients are matched to these quantities order by order in α_e , and provide the result at any given order in $1/L$ as an expansion in α_e .

shift of

$$\begin{aligned}\delta m_\phi^{(N^3\text{LO};\tilde{\alpha},\tilde{\beta})} &= -\frac{4\pi^2}{L^4} \left(\tilde{\alpha}_E^{(\phi)} + \tilde{\beta}_M^{(\phi)} \right) \sum_{\mathbf{n} \neq \mathbf{0}} |\mathbf{n}| \\ &= -\frac{4\pi^2}{L^4} \left(\alpha_E^{(\phi)} + \beta_M^{(\phi)} \right) c_{-1} + \frac{4\pi^2 \alpha_e Q}{3m_\phi L^4} \langle r^2 \rangle_\phi c_{-1} \quad ,\end{aligned}\quad (10)$$

where the regularized sum is the same as that contributing to the energy density associated with the Casimir effect, and is $c_{-1} = -0.266596$ [49]. A similar calculation yields the contribution from the c_M operator,

$$\delta m_\phi^{(N^3\text{LO};c_M)} = +\frac{4\pi^2 \alpha_e Q}{3m_\phi L^4} \langle r^2 \rangle_\phi c_{-1} \quad . \quad (11)$$

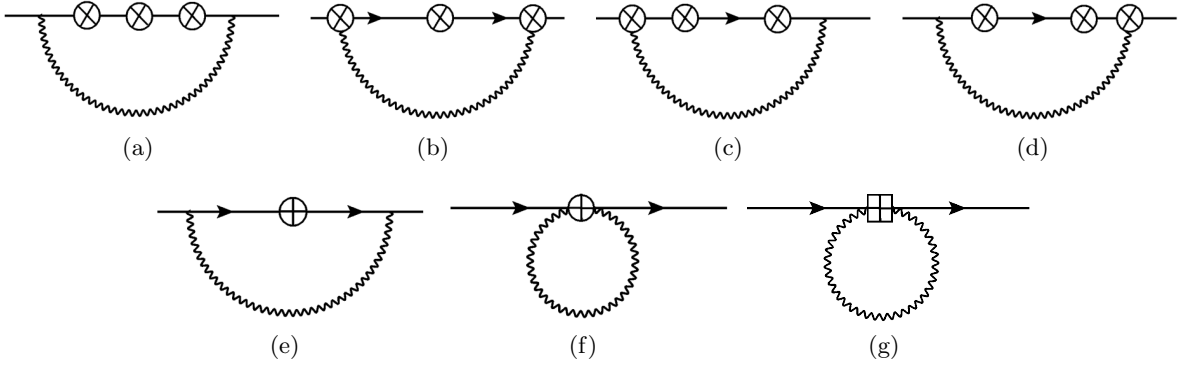


FIG. 5: One-loop diagrams contributing to the FV corrections to the mass of a scalar hadron at $N^3\text{LO}$, $\mathcal{O}(1/L^4)$. Diagrams (a-d) involve three insertions of the $|\mathbf{D}|^2/2m_\phi$ operator (crossed circles) in the scalar QED Lagrange density in Eq. (4), while (e,f) involve one insertion of the $|\mathbf{D}|^4/8m_\phi^3$ operator (the sun cross), giving a $\mathcal{O}(\alpha_e/m_\phi^3 L^4)$ correction. Diagram (g) involves an insertion of $\tilde{\alpha}_E^{(\phi)} |\mathbf{E}|^2$ and $\tilde{\beta}_M^{(\phi)} |\mathbf{B}|^2$, operators (crossed square), contributing terms of the form $\sim (\alpha_E + \beta_M)/L^4$ and $\sim \alpha_e \langle r^2 \rangle_\phi / m_\phi L^4$. A diagram analogous to (g) provides the leading contribution from the c_M operator at $\mathcal{O}(\alpha_e/m_\phi L^4)$.

Collecting the contributions up to $N^3\text{LO}$, the mass shift of a composite scalar particle in the $1/L$ expansion is

$$\delta m_\phi = \frac{\alpha_e Q^2}{2L} c_1 \left(1 + \frac{2}{m_\phi L} \right) + \frac{2\pi \alpha_e Q}{3L^3} \left(1 + \frac{4\pi}{m_\phi L} c_{-1} \right) \langle r^2 \rangle_\phi - \frac{4\pi^2}{L^4} \left(\alpha_E^{(\phi)} + \beta_M^{(\phi)} \right) c_{-1} \quad . \quad (12)$$

Therefore, for the charged and neutral pions, the mass shifts are

$$\begin{aligned}\delta m_{\pi^+} &= \frac{\alpha_e}{2L} c_1 \left(1 + \frac{2}{m_{\pi^+} L} \right) + \frac{2\pi \alpha_e}{3L^3} \left(1 + \frac{4\pi}{m_{\pi^+} L} c_{-1} \right) \langle r^2 \rangle_{\pi^+} - \frac{4\pi^2}{L^4} \left(\alpha_E^{(\pi^+)} + \beta_M^{(\pi^+)} \right) c_{-1}, \\ \delta m_{\pi^0} &= -\frac{4\pi^2}{L^4} \left(\alpha_E^{(\pi^0)} + \beta_M^{(\pi^0)} \right) c_{-1} \quad ,\end{aligned}\quad (13)$$

where potential complications due to the electromagnetic decay of the π^0 via the anomaly have been neglected. The shifts of the charged and neutral kaons have the same form, with $m_{\pi^{\pm,0}} \rightarrow m_{K^{\pm,0}}$, $\langle r^2 \rangle_{\pi^+} \rightarrow \langle r^2 \rangle_{K^+}$, $\alpha_E^{(\pi^{\pm,0})} \rightarrow \alpha_E^{(K^{\pm,0})}$ and $\beta_E^{(\pi^{\pm,0})} \rightarrow \beta_E^{(K^{\pm,0})}$. With the experimental constraints

on the charge radii and polarizabilities of the pions and kaons, numerical estimates of the FV corrections can be performed at N³LO. The LO and NLO contributions are dictated by only the charge and mass of the meson. The N²LO contribution depends upon the charge and charge radius, which, for the charged mesons, are known experimentally to be [52],

$$\sqrt{\langle r^2 \rangle}_{\pi^+} = 0.672 \pm 0.008 \text{ fm} \quad , \quad \sqrt{\langle r^2 \rangle}_{K^+} = 0.560 \pm 0.031 \text{ fm} . \quad (14)$$

The N³LO contribution from the electric and magnetic polarizabilities of the mesons depends upon their sum. The Baldin sum rule determines the charged pion combination, while the result of a two-loop χ PT calculation is used for the neutral pion combination [53],

$$\alpha_E^{(\pi^+)} + \beta_M^{(\pi^+)} = (0.39 \pm 0.04) \times 10^{-4} \text{ fm}^3 \quad , \quad \alpha_E^{(\pi^0)} + \beta_M^{(\pi^0)} = (1.1 \pm 0.3) \times 10^{-4} \text{ fm}^3 . \quad (15)$$

Unfortunately, little is known about the polarizabilities of the kaons, and so naive dimensional analysis is used to provide an estimate of their contribution [53], $\alpha_E^{(K^+)} + \beta_M^{(K^+)}$, $\alpha_E^{(K^0)} + \beta_M^{(K^0)} = (1 \pm 1) \times 10^{-4} \text{ fm}^3$. With these values, along with their experimentally measured masses, the expected FV corrections to the charged meson masses are shown in Fig. 6 and to the neutral meson masses in Fig. 7.⁸

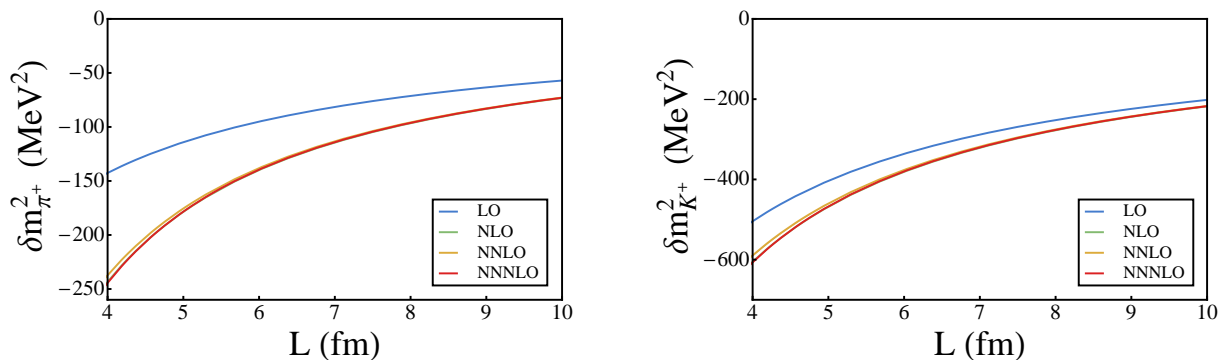


FIG. 6: The FV QED correction to the mass squared of a charged pion (left panel) and kaon (right panel) at rest in a FV at the physical meson mass. The leading contribution is due to their electric charge, and scales as $1/L$. The 1σ -uncertainty bands associated with each order in the expansion are determined from the uncertainties in the experimental and theoretical inputs.

In a volume with $L = 4$ fm, the FV QED mass shift of a charged meson is approximately 0.5 MeV. Figure 6 shows that for volumes with $L \gtrsim 4$ fm, the meson charge is responsible for essentially all of the FV modifications, with their compositeness making only a small contribution, i.e. the differences between the NLO and N²LO mass shifts are small. For the neutral mesons, the contribution from the polarizabilities is very small, but with substantial uncertainty. It is worth re-emphasizing that in forming these estimates of the QED power-law corrections, exponential corrections of the form $e^{-m_\pi L}$ have been neglected.

⁸ When comparing with previous results one should note that the squared mass shift of the π^+ , as an example, due to FV QED is

$$\delta m_{\pi^+}^2 = (m_{\pi^+} + \delta m_{\pi^+})^2 - m_{\pi^+}^2 = 2m_{\pi^+} \delta m_{\pi^+} + \mathcal{O}(\alpha_e^2) ,$$

As is evident, the leading contribution to the mass squared scales as $1/L$, contrary to a recent suggestion in the literature [10] of $1/L^2$. Note that the quantity shown in Fig. 6 and Fig. 7 is δm_ϕ^2 as opposed to δm_ϕ , as it is this

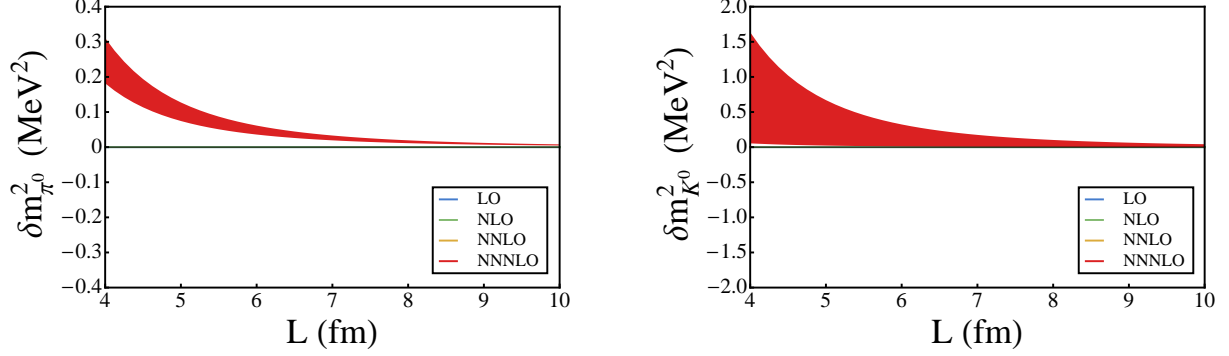


FIG. 7: The FV QED correction to the mass squared of a neutral pion (left panel) and kaon (right panel) at rest in a FV at the physical pion mass. The leading contributions are from their polarizabilities, and scale as $1/L^4$. The 1σ -uncertainty bands associated with each order in the expansion are determined from the uncertainties in the experimental and theoretical inputs.

IV. NRQED FOR THE BARYONS AND $J = \frac{1}{2}$ NUCLEI

In the case of baryons and $J = \frac{1}{2}$ nuclei, the method for determining the FV QED corrections is analogous to that for the mesons, described in the previous section, but modified to include the effects of spin and the reduction from a four-component to a two-component spinor. The low-energy EFT describing the interactions between the nucleons and the electromagnetic field is NRQED, but enhanced to include the compositeness of the nucleon. A nice review of NRQED, including the contributions from the non point-like structure of the nucleon, can be found in Ref. [54], and the relevant terms in the NRQED Lagrange density for a $N^3\text{LO}$ calculation are [19–26, 28, 45, 51, 54]

$$\begin{aligned}
\mathcal{L}_\psi = \psi^\dagger \left[& iD_0 + \frac{|\mathbf{D}|^2}{2M_\psi} + \frac{|\mathbf{D}|^4}{8M_\psi^3} + c_F \frac{e}{2M_\psi} \boldsymbol{\sigma} \cdot \mathbf{B} + c_D \frac{e}{8M_\psi^2} \boldsymbol{\nabla} \cdot \mathbf{E} \right. \\
& + ic_S \frac{e}{8M_\psi^2} \boldsymbol{\sigma} \cdot (\mathbf{D} \times \mathbf{E} - \mathbf{E} \times \mathbf{D}) + 2\pi \tilde{\alpha}_E^{(\psi)} |\mathbf{E}|^2 + 2\pi \tilde{\beta}_M^{(\psi)} |\mathbf{B}|^2 \\
& + e c_{W_1} \frac{\{\mathbf{D}^2, \boldsymbol{\sigma} \cdot \mathbf{B}\}}{8M_\psi^3} - e c_{W_2} \frac{D^i \boldsymbol{\sigma} \cdot \mathbf{B} D^i}{4M_\psi^3} \\
& \left. + e c_{p'p} \frac{\boldsymbol{\sigma} \cdot \mathbf{D} \mathbf{B} \cdot \mathbf{D} + \mathbf{B} \cdot \mathbf{D} \boldsymbol{\sigma} \cdot \mathbf{D}}{8M_\psi^3} + ie c_M \frac{\{D^i, (\boldsymbol{\nabla} \times \mathbf{B})^i\}}{8M_\psi^3} + \dots \right] \psi,
\end{aligned} \tag{16}$$

where $c_F = Q + \kappa_\psi + \mathcal{O}(\alpha_e)$ is the coefficient of the magnetic-moment interaction, with κ_ψ related to the anomalous magnetic moment of ψ , $c_D = Q + \frac{4}{3}M_\psi^2 \langle r^2 \rangle_\psi + \mathcal{O}(\alpha_e)$ contains the leading charge-radius contribution, $c_S = 2c_F - Q$ is the coefficient of the spin-orbit interaction and $c_M = (c_D - c_F)/2$. The coefficients of the $|\mathbf{E}|^2$ and $|\mathbf{B}|^2$ terms contain the polarizabilities, $1/M_\psi$ and $1/M_\psi^3$ corrections,

$$\tilde{\alpha}_E^{(\psi)} = \alpha_E^{(\psi)} - \frac{\alpha_e}{4M_\psi^3} (Q^2 + \kappa_\psi^2) - \frac{\alpha_e Q}{3M_\psi} \langle r^2 \rangle_\psi, \quad \tilde{\beta}_M^{(\psi)} = \beta_M^{(\psi)} + \frac{\alpha_e Q^2}{4M_\psi^3}. \tag{17}$$

that enters into the determination of the light-quark masses from LQCD calculations.

The operators with coefficients c_{W_1} , c_{W_2} and $c_{p'p}$, given in Ref. [54], do not contribute to the FV corrections at this order. The ellipses denote terms that are higher orders in $1/M_\psi$ and $1/\Lambda_\chi$. Two insertions of the magnetic-moment operator provide its leading contribution, as shown in Fig. 8, giving rise to $\mathcal{O}(\alpha_e/L^3)$ corrections to the mass of spin- $\frac{1}{2}$ particles. Without replicating the detail

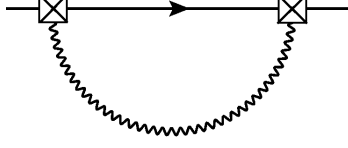


FIG. 8: The N²LO, $\mathcal{O}(\alpha_e/M_\psi^2 L^3)$, FV QED correction to the mass of a baryon from its magnetic moment. The crossed square denotes an insertion of the magnetic moment operator given in Eq. (16).

presented in the previous section, the sum of the contributions to the FV self-energy modification of a composite fermion, up to N³LO, is

$$\begin{aligned} \delta M_\psi &= \frac{\alpha_e Q^2}{2L} c_1 \left(1 + \frac{2}{M_\psi L}\right) + \frac{2\pi\alpha_e Q}{3L^3} \langle r^2 \rangle_\psi + \frac{\pi\alpha_e}{M_\psi^2 L^3} \left[\frac{1}{2} Q^2 + (Q + \kappa_\psi)^2 \right] \\ &\quad - \frac{4\pi^2}{L^4} \left(\tilde{\alpha}_E^{(\psi)} + \tilde{\beta}_M^{(\psi)} \right) c_{-1} + \frac{\pi^2 \alpha_e Q}{M_\psi^3 L^4} \left(\frac{4}{3} M_\psi^2 \langle r^2 \rangle_\psi - \kappa_\psi \right) c_{-1} - \frac{\alpha_e \pi^2}{M_\psi^3 L^4} \kappa_\psi (Q + \kappa_\psi) c_{-1}. \end{aligned} \quad (18)$$

Therefore, for the proton and neutron, the FV QED mass shifts are

$$\begin{aligned} \delta M_p &= \frac{\alpha_e}{2L} c_1 \left(1 + \frac{2}{M_p L}\right) + \frac{2\pi\alpha_e}{3L^3} \left(1 + \frac{4\pi}{M_p L} c_{-1}\right) \langle r^2 \rangle_p + \frac{\pi\alpha_e}{M_p^2 L^3} \left(\frac{1}{2} + (1 + \kappa_p)^2 \right) \\ &\quad - \frac{4\pi^2}{L^4} \left(\alpha_E^{(p)} + \beta_M^{(p)} \right) c_{-1} - \frac{2\pi^2 \alpha_e \kappa_p}{M_p^3 L^4} c_{-1}, \\ \delta M_n &= \kappa_n^2 \frac{\pi\alpha_e}{M_n^2 L^3} - \frac{4\pi^2}{L^4} \left(\alpha_E^{(n)} + \beta_M^{(n)} \right) c_{-1}, \end{aligned} \quad (19)$$

where the anomalous magnetic moments of the proton and neutron give $\kappa_p = 1.792847356(23)$ and $\kappa_n = -1.9130427(5)M_n/M_p$, respectively [52]. One of the N²LO contributions to the proton FV QED correction depends upon its charge radius, which is known experimentally to be, $\langle r^2 \rangle_p = 0.768 \pm 0.012 \text{ fm}^2$ [52]. Further, part of the N³LO contribution depends upon the electric and magnetic polarizabilities, which are constrained by the Baldin sum rule, [53]

$$\alpha_E^{(p)} + \beta_M^{(p)} = (13.69 \pm 0.14) \times 10^{-4} \text{ fm}^3, \quad \alpha_E^{(n)} + \beta_M^{(n)} = (15.2 \pm 0.5) \times 10^{-4} \text{ fm}^3. \quad (20)$$

With these values for the properties of the proton and neutron, along with their experimentally measured masses, the expected FV modifications to their masses are shown in Fig. 9.

The proton FV QED corrections are consistent with those of the charged scalar mesons. However, the neutron corrections, while very small, of the order of a few keVs, exhibit more structure. The N²LO contribution from the magnetic moment increases the mass in FV, scaling as $1/M_n^2 L^3$, similar to the polarizabilities which make a positive contribution and scale as $1/L^4$ (N³LO). Note that the polarizabilities of the nucleon are dominated by the response of the pion cloud, while the magnetic moments are dominated by physics at the chiral symmetry breaking scale. Further the magnetic-moment contributions are suppressed by two powers of the nucleon mass.

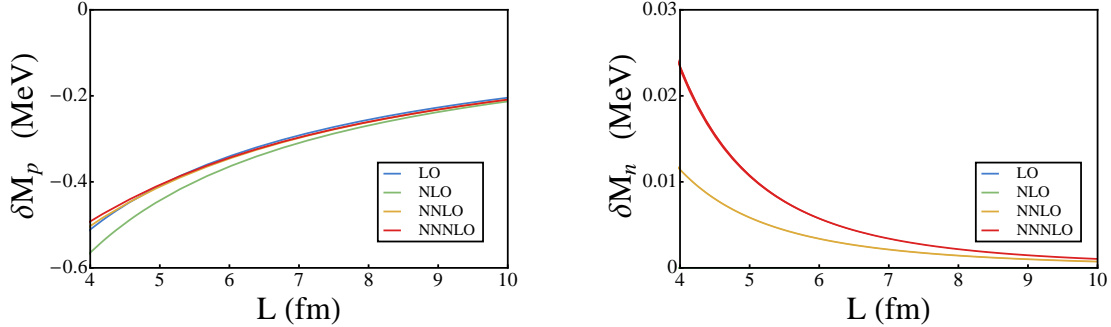


FIG. 9: The FV QED correction to the mass of the proton (left panel) and neutron (right panel) at rest in a FV at the physical pion mass. The leading contribution to the proton mass shift is due to its electric charge, and scales as $1/L$, while the leading contribution to the neutron mass shift is due to its magnetic moment, and scales as $1/L^3$. The $1 - \sigma$ uncertainty bands associated with each order in the expansion are determined from the uncertainties in the experimental and theoretical inputs.

There is an interesting difference between the meson and baryon FV modifications. As the nucleon mass is approximately seven times the pion mass, and twice the kaon mass, the recoil corrections are suppressed compared with those of the mesons. Further, the nucleons are significantly “softer” than the mesons, as evidenced by their polarizabilities. However, the NLO recoil corrections to the proton mass are of approximately the same size as the N²LO structure contributions, as seen in Fig. 9.

V. NUCLEI

A small number of LQCD collaborations have been calculating the binding of light nuclei and hypernuclei at unphysical light-quark masses in the isospin limit and without QED [55–64]. However, it is known that as the atomic number of a nucleus increases, the Coulomb energy increases with the square of its charge, and significantly reduces the binding of large nuclei. The simplest nucleus is the deuteron, but as it is weakly bound at the physical light-quark masses, and consequently unnaturally large, it is likely that it will be easier for LQCD collaborations to compute other light nuclei, such as ${}^4\text{He}$, rather than the deuteron.

A NREFT for vector QED shares the features of the NREFTs for scalars and fermions that are relevant for the current analysis. One difference is in the magnetic moment contribution, and another is the contribution from the quadrupole interaction. The FV corrections to the deuteron mass and binding energy, δB_d , are shown in Fig. 10, where the experimentally determined charge radius, magnetic moment and polarizabilities have been used. Due to the large size of the deuteron, and its large polarizability, the $1/L$ expansion converges slowly in modest volumes, and it appears that $L \gtrsim 12$ fm is required for a reliable determination of the QED FV effects, consistent with the size of volumes required to extract the binding and S-matrix parameters of the deuteron in the absence of QED [65]. The QED FV corrections to the deuteron binding energy are seen to be significantly smaller than its total energy in large volumes, largely because the leading contribution to the deuteron and to the proton cancel. As the deuteron has spin and parity of $J^\pi = 1^+$, it also possesses a quadrupole moment which contributes to the FV QED effects at $\mathcal{O}(1/L^5)$ through two insertions.

The NREFTs used to study the FV contributions to the mass of the pions in the previous section also apply to the ${}^4\text{He}$ nucleus, and the FV corrections to the mass of ${}^4\text{He}$ and its binding energy, $\delta B_{{}^4\text{He}}$, are shown in Fig. 11. Unlike the deuteron, the leading FV corrections to ${}^4\text{He}$ do

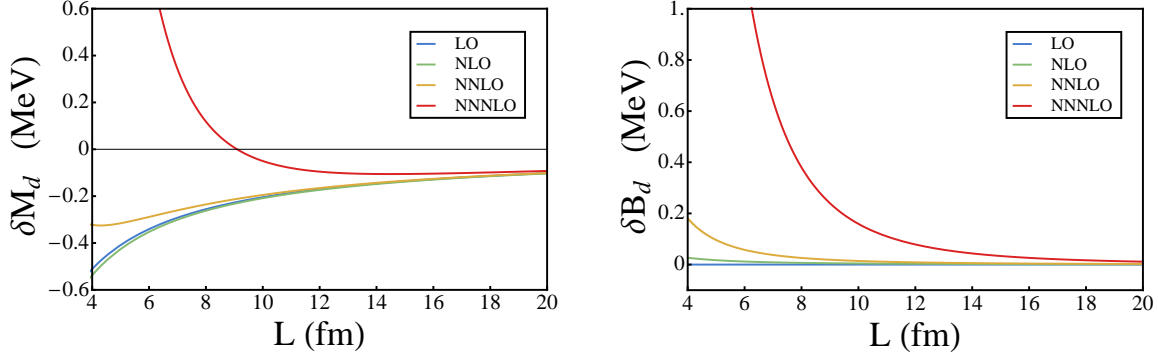


FIG. 10: The left panel shows the FV QED correction to the mass of the deuteron at rest in a FV at the physical pion mass. The leading contribution is from its electric charges, and scales as $1/L$. The right panel shows the FV QED correction to the deuteron binding energy for which the $1/L$ contributions cancel. The 1σ -uncertainty bands associated with each order in the expansion are determined from the uncertainties in the experimental and theoretical inputs.

not cancel in the binding energy due to the interactions between the two protons, but are reduced by a factor of two.

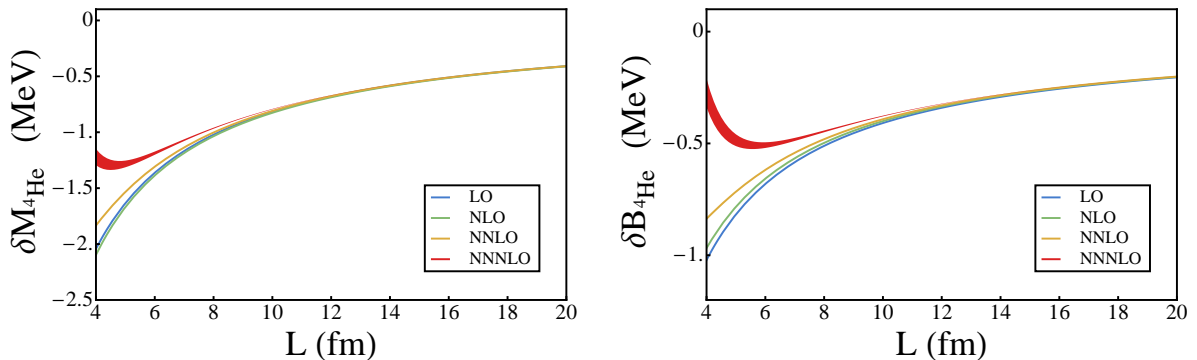


FIG. 11: The left panel shows the FV QED correction to the mass of ${}^4\text{He}$ at rest in a FV at the physical pion mass. The leading contribution is from its electric charge, and scales as $1/L$. The right panel shows the FV QED correction to the ${}^4\text{He}$ binding energy. The uncertainty bands associated with each order in the expansion are determined from the uncertainties in the experimental and theoretical inputs.

VI. ANOMALOUS MAGNETIC MOMENT OF THE MUON

Experimental and theoretical determinations of the anomalous magnetic moment of the muon are providing a stringent test of the Standard Model of particle physics. The current discrepancy between the theoretical [66, 67] and experimental determinations [68], at the level of 2.9 to 3.6 σ , but not 5σ , cannot yet be interpreted as a signal of new physics. As upcoming experiments, Fermilab E989 and J-PARC E34, plan to reduce the experimental uncertainty down to 0.14 ppm, theoretical calculations of non-perturbative hadronic contributions must be refined in the short term. LQCD is expected to contribute to improving the theoretical prediction of the standard model, and several recent efforts have been directed at obtaining the hadronic vacuum-polarization and hadronic light-by-light contributions to the muon $g - 2$ [69–79]. Theoretical challenges facing these calculations have been identified and will be addressed during the next few years.

Here we show that the most naive scheme to obtain the magnetic moment of the muon by a direct calculation has volume effects that scale as $\mathcal{O}(\alpha_e/(m_\mu L))$, requiring unrealistically large volumes to achieve the precision required to be sensitive to new physics. A detailed exploration of the issues related to extracting matrix elements of the electromagnetic current from LQCD calculations can be found in Ref. [80]. Although it might appear that the leading contribution to the FV modification of the magnetic moment of the muon in NRQED will arise from one-loop diagrams involving one insertion of the the magnetic moment operator, such contributions vanish. In fact, the leading $1/(m_\mu L)$ FV correction comes from the tree-level insertion of the magnetic-moment operator multiplied by a factor of E/m_μ , where E is the energy of the muon, giving rise to, at $\mathcal{O}(\alpha_e)$,

$$\kappa_\mu \equiv \frac{g_\mu - 2}{2} = \frac{\alpha_e}{2\pi} \left[1 + \frac{\pi c_1}{m_\mu L} + \mathcal{O}\left(\frac{1}{m_\mu^2 L^2}\right) \right]. \quad (21)$$

The factor of E/m_μ arises in matching the NR theory to QED [26], in which each external leg in the NR theory must be accompanied by a factor of $\sqrt{\frac{E}{m_\mu}}$. Since $E = m_\mu + \frac{e^2}{8\pi} \frac{c_1}{L} + \dots$, it can be readily seen that the effective tree-level vertex multiplied by this normalization factor results in the κ_μ given in Eq. (21). This contribution is present in the LO QED contribution to the anomalous magnetic moment (Schwinger term) when calculated in a cubic FV with PBCs and the photon zero mode removed.

To better understand the severity of the volume corrections to such a naive calculation, it is sufficient to note that in order to reduce the FV correction to 1 ppm (comparable to the current experimental error), a volume of $\sim (60 \text{ nm})^3$ is required. In the largest volumes that will be available to LQCD+QED calculations in the near future, with $L \lesssim 10 \text{ fm}$, the FV corrections to a direct calculation of the muon magnetic moment will flip the sign of the anomalous magnetic moment. It is important to note that lattice practitioners are not attempting direct calculations of the muon $g-2$, but rather are isolating the hadronic contributions, which have enormously smaller FV effects compared to the one we have identified. In some sense, the result we have presented in this section is for entertainment purposes only.

VII. LATTICE ARTIFACTS

The results that we have presented in the previous sections have assumed a continuous spacetime, and have not yet considered the impact of a finite lattice spacing. With the inclusion of QED, there are two distinct sources of lattice spacing artifacts that will modify the FV QED corrections we have considered. The coefficients of each of the higher dimension operators in the NREFTs will receive lattice spacing corrections, and for an $\mathcal{O}(a)$ -improved action (a is the lattice spacing) they are a polynomial in powers of a of the form $d_i \sim d_{i0} + d_{i2}a^2 + d_{i3}a^3 + \dots$. The coefficients d_{ij} are determined by the strong interaction dynamics and the particular discretizations used in a given calculation. In addition, the electromagnetic interaction will be modified in analogy with the strong sector, giving rise to further lattice spacing artifacts in the matching conditions between the full and the NR theories, and also in the value of one-loop diagrams⁹. For an improved action, the naive expectation is that such correction will first appear, beyond the trivial correction from the modified hadron mass in the NLO term, at $\alpha_e a^2/L^3$ in the $1/L$ expansion. They are a N²LO

⁹ The lattice artifacts will depend upon whether the compact or non-compact formulation of QED is employed - the former inducing non-linearities in the electromagnetic field which vanish in the continuum limit. The discussions we present in this section apply to both the compact and non-compact formulations.

contribution arising from modifications to the one-loop Coulomb self-energy diagram. This is the same order as contributions from the charge radius, recoil corrections and the magnetic moment, which are found to make a small contribution to the mass shift in modest lattice volumes. As the lattice spacing is small compared to the size of the proton and the inverse mass of the proton, these lattice artifacts are expected to provide a small modification to the N²LO terms we have determined. In addition, there are operators in the Symanzik action [81–83] that violate Lorentz symmetry as the calculations are performed on an underlying hypercubic grid. Such operators require the contraction of at least four Lorentz vectors in order to form a hypercubically-invariant, but Lorentz-violating, operator, for instance three derivatives and one electromagnetic field, or four derivatives. The suppression of Lorentz-violating contributions at small lattice spacings, along with smearing, has been discussed in Ref. [84].

A second artifact arises from the lattice volume. The NREFTs are constructed as an expansion in derivatives acting on fields near their classical trajectory. As emphasized by Tiburzi [80] and others, this leads to modifications in calculated matrix elements because derivatives are approximated by finite differences in lattice calculations. For large momenta, this is a small effect because of the large density of states, but at low momenta, particularly near zero, this can be a non-negligible effect that must be accounted for. This leads to a complication in determining, for instance, magnetic moments from the forward limit of a form factor, relevant to the discussion in the previous section. However, this does not impact the present calculations of FV QED corrections to the masses of the mesons, baryons and nuclei.

VIII. CONCLUSIONS

For Lattice QCD calculations performed in volumes that are much larger than the inverse pion mass, the finite-volume electromagnetic corrections to hadron masses can be calculated systematically using a NREFT. The leading two orders in the $1/L$ expansion for mesons have been previously calculated using chiral perturbation theory, and depend only upon their electric charge and mass. We have shown that these two orders are universal FV QED corrections to the mass of charged particles. Higher orders in the expansion are determined by recoil corrections and by the structure of the hadron, such as its electromagnetic multipole moments and polarizabilities, which we calculate using a NREFT. One advantage enjoyed by the NREFT is that the coefficients of the operators in the Lagrange density are directly related to the structure of the hadron, order by order in α_e , as opposed to being perturbative approximations as computed, for instance, in χ PT. For the mesons and baryons, the FV QED effects associated with their structure, beyond their charge, are found to be small even in modest lattice volumes. For nuclei, as long as the volume is large enough so that the non-QED effects are exponentially small, dictated by the nuclear radius, their charge dominates the FV QED corrections, with only small modifications due to the structure of the nucleus.

Acknowledgments

We would like to thank Silas Beane, Michael Buchoff, Emmanuel Chang and Sanjay Reddy for interesting discussions. We were supported in part by the DOE grant No. DE-FG02-97ER41014

and by DOE grant No. DE-FG02-00ER41132.

-
- [1] S. Aoki et al. (PACS-CS Collaboration), Phys.Rev. **D81**, 074503 (2010), 0911.2561.
 - [2] S. Durr, Z. Fodor, C. Hoelbling, S. Katz, S. Krieg, et al., Phys.Lett. **B701**, 265 (2011), 1011.2403.
 - [3] R. Arthur et al. (RBC Collaboration, UKQCD Collaboration), Phys.Rev. **D87**, 094514 (2013), 1208.4412.
 - [4] S. Aoki, K. Ishikawa, N. Ishizuka, K. Kanaya, Y. Kuramashi, et al., Phys.Rev. **D86**, 034507 (2012), 1205.2961.
 - [5] S. Durr, Z. Fodor, C. Hoelbling, S. Krieg, T. Kurth, et al. (2013), 1310.3626.
 - [6] T. Blum, T. Doi, M. Hayakawa, T. Izubuchi, and N. Yamada, Phys.Rev. **D76**, 114508 (2007), 0708.0484.
 - [7] S. Basak et al. (MILC Collaboration), PoS **LATTICE2008**, 127 (2008), 0812.4486.
 - [8] T. Blum, R. Zhou, T. Doi, M. Hayakawa, T. Izubuchi, et al., Phys.Rev. **D82**, 094508 (2010), 1006.1311.
 - [9] A. Portelli et al. (Budapest-Marseille-Wuppertal Collaboration), PoS **LATTICE2010**, 121 (2010), 1011.4189.
 - [10] A. Portelli, S. Durr, Z. Fodor, J. Frison, C. Hoelbling, et al., PoS **LATTICE2011**, 136 (2011), 1201.2787.
 - [11] G. de Divitiis, R. Frezzotti, V. Lubicz, G. Martinelli, R. Petronzio, et al., Phys.Rev. **D87**, 114505 (2013), 1303.4896.
 - [12] S. Borsanyi, S. Durr, Z. Fodor, J. Frison, C. Hoelbling, et al., Phys.Rev.Lett. **111**, 252001 (2013), 1306.2287.
 - [13] S. Drury, T. Blum, M. Hayakawa, T. Izubuchi, C. Sachrajda, et al. (2013), 1312.0477.
 - [14] S. Borsanyi, S. Durr, Z. Fodor, C. Hoelbling, S. Katz, et al. (2014), 1406.4088.
 - [15] E. Hilf and L. Polley, Physics Letters B **131**, 412 (1983), ISSN 0370-2693.
 - [16] A. Duncan, E. Eichten, and H. Thacker, Phys.Rev.Lett. **76**, 3894 (1996), hep-lat/9602005.
 - [17] M. Hayakawa and S. Uno, Prog.Theor.Phys. **120**, 413 (2008), 0804.2044.
 - [18] W. A. Bardeen, J. Bijnens, and J.-M. Gérard, Phys. Rev. Lett. **62**, 1343 (1989).
 - [19] N. Isgur and M. B. Wise, Phys.Lett. **B232**, 113 (1989).
 - [20] N. Isgur and M. B. Wise, Phys.Lett. **B237**, 527 (1990).
 - [21] E. E. Jenkins and A. V. Manohar, Phys.Lett. **B255**, 558 (1991).
 - [22] E. E. Jenkins and A. V. Manohar, Effective field theories of the standard model. Proceedings, Workshop, Dobogoko, Hungary, August 22-26, 1991 (1991).
 - [23] B. Thacker and G. P. Lepage, Phys.Rev. **D43**, 196 (1991).
 - [24] P. Labelle (1992), hep-ph/9209266.
 - [25] A. V. Manohar, Phys.Rev. **D56**, 230 (1997), hep-ph/9701294.
 - [26] M. E. Luke and M. J. Savage, Phys.Rev. **D57**, 413 (1998), hep-ph/9707313.
 - [27] R. J. Hill and G. Paz, Phys.Rev.Lett. **107**, 160402 (2011), 1103.4617.
 - [28] J.-W. Chen, G. Rupak, and M. J. Savage, Nucl.Phys. **A653**, 386 (1999), nucl-th/9902056.
 - [29] D. B. Kaplan, M. J. Savage, and M. B. Wise, Phys.Lett. **B424**, 390 (1998), nucl-th/9801034.
 - [30] D. B. Kaplan, M. J. Savage, and M. B. Wise, Nucl.Phys. **B534**, 329 (1998), nucl-th/9802075.
 - [31] M. Butler and J.-W. Chen, Nucl.Phys. **A675**, 575 (2000), nucl-th/9905059.
 - [32] M. Butler, J.-W. Chen, and X. Kong, Phys.Rev. **C63**, 035501 (2001), nucl-th/0008032.
 - [33] M. Butler and J.-W. Chen, Phys.Lett. **B520**, 87 (2001), nucl-th/0101017.
 - [34] G. Martinelli, G. Parisi, R. Petronzio, and F. Rapuano, Phys.Lett. **B116**, 434 (1982).
 - [35] H. Fiebig, W. Wilcox, and R. Woloshyn, Nucl.Phys. **B324**, 47 (1989).
 - [36] C. W. Bernard, T. Draper, K. Olynyk, and M. Rushton, Phys.Rev.Lett. **49**, 1076 (1982).
 - [37] F. Lee, R. Kelly, L. Zhou, and W. Wilcox, Phys.Lett. **B627**, 71 (2005), hep-lat/0509067.
 - [38] J. C. Christensen, W. Wilcox, F. X. Lee, and L.-m. Zhou, Phys.Rev. **D72**, 034503 (2005), hep-lat/0408024.
 - [39] F. X. Lee, L. Zhou, W. Wilcox, and J. C. Christensen, Phys.Rev. **D73**, 034503 (2006), hep-lat/0509065.
 - [40] M. Engelhardt (LHPC Collaboration), Phys.Rev. **D76**, 114502 (2007), 0706.3919.
 - [41] W. Detmold, B. C. Tiburzi, and A. Walker-Loud, Phys.Rev. **D79**, 094505 (2009), 0904.1586.
 - [42] A. Alexandru and F. X. Lee, PoS **LAT2009**, 144 (2009), 0911.2520.

- [43] W. Detmold, B. Tiburzi, and A. Walker-Loud, Phys.Rev. **D81**, 054502 (2010), 1001.1131.
- [44] T. Primer, W. Kamleh, D. Leinweber, and M. Burkardt (2013), 1307.1509.
- [45] J.-W. Lee and B. C. Tiburzi (2013), 1312.3969.
- [46] A. Castro, A. Rubio, and M. J. Stott, ArXiv Physics e-prints (2000), physics/0012024.
- [47] A. S. Kronfeld and U. Wiese, Nucl.Phys. **B401**, 190 (1993), hep-lat/9210008.
- [48] M. Luscher, Commun.Math.Phys. **105**, 153 (1986).
- [49] P. Hasenfratz and H. Leutwyler, Nucl.Phys. **B343**, 241 (1990).
- [50] M. Luscher, Nucl.Phys. **B354**, 531 (1991).
- [51] S. R. Beane, W. Detmold, T. C. Luu, K. Orginos, M. J. Savage, et al., Phys.Rev.Lett. **100**, 082004 (2008), 0710.1827.
- [52] J. Beringer et al. (Particle Data Group), Phys.Rev. **D86**, 010001 (2012).
- [53] B. R. Holstein and S. Scherer (2013), 1401.0140.
- [54] R. J. Hill, G. Lee, G. Paz, and M. P. Solon, Phys.Rev. **D87**, 053017 (2013), 1212.4508.
- [55] S. R. Beane et al. (NPLQCD Collaboration), Phys.Rev. **D81**, 054505 (2010), 0912.4243.
- [56] T. Yamazaki, Y. Kuramashi, and A. Ukawa (PACS-CS Collaboration), Phys.Rev. **D81**, 111504 (2010), 0912.1383.
- [57] S. Beane et al. (NPLQCD Collaboration), Phys.Rev.Lett. **106**, 162001 (2011), 1012.3812.
- [58] T. Inoue et al. (HAL QCD Collaboration), Phys.Rev.Lett. **106**, 162002 (2011), 1012.5928.
- [59] T. Inoue (HAL QCD Collaboration), AIP Conf.Proc. **1441**, 335 (2012), 1109.1620.
- [60] S. Beane et al. (NPLQCD Collaboration), Phys.Rev. **D85**, 054511 (2012), 1109.2889.
- [61] T. Yamazaki, Y. Kuramashi, and A. Ukawa (Collaboration for the PACS-CS), Phys.Rev. **D84**, 054506 (2011), 1105.1418.
- [62] T. Yamazaki, K.-i. Ishikawa, Y. Kuramashi, and A. Ukawa, Phys.Rev. **D86**, 074514 (2012), 1207.4277.
- [63] T. Yamazaki, K.-i. Ishikawa, Y. Kuramashi, and A. Ukawa, PoS **LATTICE2012**, 143 (2012), 1211.4334.
- [64] S. Beane, E. Chang, S. Cohen, W. Detmold, H. Lin, et al., Phys.Rev. **D87**, 034506 (2013), 1206.5219.
- [65] R. A. Briceño, Z. Davoudi, T. Luu, and M. J. Savage, Phys.Rev. **D88**, 114507 (2013), 1309.3556.
- [66] T. Aoyama, M. Hayakawa, T. Kinoshita, and M. Nio, Phys.Rev.Lett. **109**, 111808 (2012), 1205.5370.
- [67] C. Gnendiger, D. Stockinger, and H. Stockinger-Kim, Phys.Rev. **D88**, 053005 (2013), 1306.5546.
- [68] G. Bennett et al. (Muon G-2 Collaboration), Phys.Rev. **D73**, 072003 (2006), hep-ex/0602035.
- [69] M. Della Morte, B. Jager, A. Juttner, and H. Wittig, JHEP **1203**, 055 (2012), 1112.2894.
- [70] X. Feng, K. Jansen, M. Petschlies, and D. B. Renner, Phys.Rev.Lett. **107**, 081802 (2011), 1103.4818.
- [71] P. Boyle, L. Del Debbio, E. Kerrane, and J. Zanotti, Phys.Rev. **D85**, 074504 (2012), 1107.1497.
- [72] X. Feng, G. Hotzel, K. Jansen, M. Petschlies, and D. B. Renner, PoS **LATTICE2012**, 174 (2012), 1211.0828.
- [73] T. Blum, M. Hayakawa, and T. Izubuchi, PoS **LATTICE2012**, 022 (2012), 1301.2607.
- [74] C. Aubin, T. Blum, M. Golterman, K. Maltman, and S. Peris (2013), 1311.5504.
- [75] F. Burger, X. Feng, G. Hotzel, K. Jansen, M. Petschlies, et al. (2013), 1308.4327.
- [76] C. Aubin, T. Blum, M. Golterman, and S. Peris, Phys.Rev. **D88**, 074505 (2013), 1307.4701.
- [77] T. Blum, A. Denig, I. Logashenko, E. de Rafael, B. Lee Roberts, et al. (2013), 1311.2198.
- [78] F. Burger, X. Feng, G. Hotzel, K. Jansen, M. Petschlies, et al., PoS **LATTICE2013**, 301 (2013), 1311.3885.
- [79] C. Aubin, T. Blum, M. Golterman, and S. Peris (2013), 1311.1078.
- [80] B. C. Tiburzi, Phys.Rev. **D77**, 014510 (2008), 0710.3577.
- [81] K. Symanzik, Nucl.Phys. **B226**, 187 (1983).
- [82] K. Symanzik, Nucl.Phys. **B226**, 205 (1983).
- [83] G. Parisi, Nucl.Phys. **B254**, 58 (1985).
- [84] Z. Davoudi and M. J. Savage, Phys.Rev. **D86**, 054505 (2012), 1204.4146.